RMetS

Royal Meteorological Society

Impacts of formaldehyde photolysis rates on tropospheric chemistry

M. C. Cooke,[1]* S. R. Utembe,[1] P. Gorrotxategi Carbajo,[1] A. T. Archibald,[1] A. J. Orr-Ewing,[1] M. E. Jenkin,[1,2] R. G. Derwent,[3] D. J. Lary[4] and D. E. Shallcross[1]

[1]*School of Chemistry, University of Bristol, Cantocks Close, Bristol BS8 1TS, UK*
[2]*Atmospheric Chemistry Services, Okehampton, Devon EX20 1FB, UK*
[3]*Rdscientific, Newbury, Berkshire, UK*
[4]*Goddard Earth Sciences and Technology Center, University of Maryland Baltimore County, Baltimore, MD, USA*

Correspondence to:
M. C. Cooke, School of Chemistry,
University of Bristol, Cantocks
Close, Bristol BS8 1TS, UK.
*E-mail: chmcc@bristol.ac.uk*

Abstract

A global chemistry transport model is employed to investigate the impact of recent laboratory determinations of photolysis parameters for formaldehyde on concentrations of tropospheric trace gases. Using the new laboratory data, the photolysis of formaldehyde is a more significant removal pathway. HO_x levels are increased with the greatest changes towards the top of the troposphere and the poles, making formaldehyde a more significant source of upper tropospheric HO_x than previously thought. Global totals of ozone and secondary organic aerosol increase with the rise in ozone being more significant at higher solar zenith angles. Copyright © 2010 Royal Meteorological Society

Keywords: formaldehyde; photolysis; global; modelling; HO_x

1. Introduction

Formaldehyde is a ubiquitous constituent of the troposphere that is produced by direct emission from fossil fuel consumption and biomass burning and as a product in the oxidation of volatile organic compounds. Removal from the atmosphere is via reaction with the hydroxyl radical (OH) $\{k(298 \text{ K}) = 8.5 \times 10^{-12} \text{ cm}^3 \text{ molecule}^{-1} \text{ s}^{-1}$ (Sander *et al.*, 2006)$\}$, the nitrate radical (NO_3) $\{[(k(298 \text{ K}) = 5.8 \times 10^{-16} \text{ cm}^3 \text{ molecule}^{-1} \text{ s}^{-1}$ (Sander *et al.*, 2006)$\}$ and photolysis reactions (1) and (2):

$$HCHO + hv \longrightarrow H_2 + CO \quad (1)$$

$$HCHO + hv \longrightarrow H + HCO \quad (2)$$
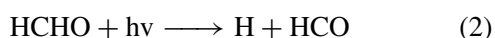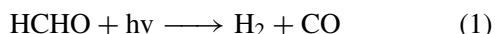
Once formed, HCO reacts rapidly with O_2 to give the hydroperoxyl radical (HO_2) and CO, and H reacts with O_2 to give HO_2. Reactions of HO_2 with O_3 and NO result in the formation of OH. Formaldehyde is thought to be a major source of OH at high-solar zenith angles because of the longer wavelength threshold of the radical channel relative to the photolysis of O_3. Formaldehyde is also of interest as a source of HO_2 and OH (usually collectively referred to as odd OHs or HO_x) in the upper troposphere (UT) (Logan *et al.*, 1981). Over the past decade it has emerged that measured HO_x in the UT exceeds that predicted by models and that a range of HO_x precursors may contribute to this discrepancy. Such precursors include formaldehyde, alkyl peroxides, acetone and isoprene derivatives that are thought to be transported from lower altitudes (Brune, 1998; Collins *et al.*, 1999;

Crawford *et al.*, 1999; Colomb *et al.*, 2006; Fried *et al.*, 2008; Jaeglé *et al.*, 2001). These studies have indicated the importance of deep tropical convection and convection from the marine boundary layer on the UT HO_x budget.

Formaldehyde is a key precursor, being formed from the degradation of most hydrocarbons and any substantial change in photolysis parameters may have a non-negligible impact on UT HO_x. The current recommended formaldehyde absorption cross-sections $[\sigma(\lambda)]$ by the NASA-JPL panel (Sander *et al.*, 2006) and the IUPAC panel (Atkinson *et al.*, 2006) were determined at a resolution of ~0.025 nm by Meller and Moortgat (2000). Measurements at a spectral resolution of 0.0032 nm have been conducted by Smith *et al.* (2006) showing a greater peak of formaldehyde cross-section in the range 300–340 nm. Direct detection of the HCO radical has been conducted by Gorrotxategi Carbajo *et al.* (2008) allowing for absolute quantum yield $[\Phi(\lambda)]$ determination for the radical channel of photolysis. These studies thus provide improved quantification of the parameters, which determine the atmospheric photolysis rate of formaldehyde, and which are likely to influence the NASA-JPL and IUPAC recommendations. In the current study a global chemistry transport model (CTM) is used to investigate the impact of these new photolysis measurements.

2. Model and simulations

The model used is an updated version of the UK Meteorological Office tropospheric CTM (STOCHEM)

described by Collins *et al.* (1997), with updates reported in detail in the recent paper of Utembe *et al.* (2009a). STOCHEM is a global three-dimensional CTM, which uses a Lagrangian approach to advect 50 000 air parcels using a fourth-order Runge-Kutta scheme with advection time steps of 3 h. The transport and radiation models are driven by archived meteorological data, generated by the Met office numerical weather prediction models as analysis fields with a resolution of $1.25°$ longitude and $0.83°$ latitude and on 12 vertical levels extending to 100 hPa. The model of Derwent *et al.* (2008) has been employed with updates to the photochemical mechanism and surface emissions as described below.

The chemistry employed is the most reduced version of the common representative intermediates mechanism (CRIv2-R5) (Jenkin *et al.*, 2008; Watson *et al.*, 2008; Utembe *et al.*, 2009b), which represents the chemistry of methane and 22 emitted non-methane hydrocarbons. Each parcel contains the concentrations of 219 species involved in 618 photolytic, gas phase and heterogeneous chemical reactions, with a 5-min chemistry time step. There are also 14 species representing the formation of secondary organic aerosol (SOA), which are derived from the oxidation of aromatic hydrocarbons, monoterpenes and isoprene (Utembe *et al.*, 2009b).

The surface emissions (man-made, biomass burning, vegetation, oceans, soil and 'other' surface emissions) are distributed using two-dimensional source maps. Emission totals for CO, NO_x and non-methane hydrocarbons are taken from the Precursor of Ozone and their Effects in the Troposphere (POET) inventory (Granier *et al.*, 2005). The emissions of aromatic species ortho-xylene, benzene and toluene were taken from Henze *et al.* (2008). Biomass burning emissions of ethyne, formaldehyde and acetic acid were produced using scaling factors from Andreae and Merlet (2001) per mole of CO emitted. NASA inventories are used for aircraft NO_x emissions for 1992 taken from Penner *et al.* (1999). The lightning and aircraft NO_x emissions are monthly averages and are three-dimensional in distribution.

Three runs were performed to investigate the effect of formaldehyde photolysis on atmospheric trace gases. The only differences between the three runs were the choice of source data for the photolysis cross-sections and quantum yields for formaldehyde. The first two runs used data from NASA-JPL recommendations in 1992 (DeMore, 1992) and 2006 (Sander *et al.*, 2006). The third-run used data from Sander *et al.* (2006), but substituted with the data of Gorrotxategi Carbajo *et al.* (2008) and Smith *et al.* (2006) over the wavelength range from 300 to 330 nm. These runs will subsequently be referred to as JPL92, JPL06 and CarJPL06, respectively. Each model run was performed for 24 months with the first 12 months being a spin-up.

Table I. Percentage removal of HCHO from the troposphere.

Reaction	JPL92 (%)	JPL06 (%)	CarJPL06 (%)
hv (radical)	23.2	33.5	38.1 (+4.6)
hv (molecular)	37.7	28.5	25.3 (−3.2)
OH	39.1	37.9	36.6 (−1.3)
NO_3	<0.1	<0.1	<0.1

Values in brackets indicate the changes between JPL06 and CarJPL06.

3. Results

Table I shows the tropospheric removal routes of formaldehyde and the proportion of each route for the three global simulations. The experimental data have developed considerably between 1992 and 2006, JPL reports because of higher resolution cross-section measurements and more accurate techniques for evaluating the quantum yield. This development has resulted in the radical channel of photolysis being recognised as a more important removal route (23.2–33.5%) with the overall removal by photolysis also being more significant (60.9–62.0%).

The remainder of the discussion will look at the differences between the current recommended values by Sander *et al.* (2006) (run JPL06) and the incorporation of the data of Gorrotxategi Carbajo *et al.* (2008) (run CarJPL06). A high-resolution UV radiation model was used by Gorrotxategi Carbajo *et al.* (2008) to calculate $J(HCO)$ increases of $25-30\ (\pm15)\%$ between 300 and 330 nm. Table I shows that the radical channel has become a more significant removal route (increase of 4.6%), and overall photolysis is a more dominant removal process (62.0–63.4%). The increased importance of the radical channel results in an increase in the concentration of both HO_2 and OH, with the later increasing by 1.5% on a globally averaged basis (Table II). The increase in OH causes the emitted VOCs and CO to be removed more rapidly from the troposphere thus the concentration of these species has reduced on a global scale, as presented in Table II.

Table II. The mass and percentage changes for some of the main species.

Compound	GB (JPL06) – GB (CarJPL06) (Gg)	GB % change
CO	-2.57×10^3	−0.74
O_3	8.14×10^1	0.03
H_2	-3.52×10^3	−2.50
OH	3.88×10^{-3}	1.41
HO_2	6.69×10^{-1}	2.51
HCHO	-4.42×10^1	−4.49
NO_x	-1.97×10^{-3}	−3.29
CH_4	-8.0×10^3	−0.21
C_2H_6	-1.73×10^1	−1.28
C_6H_6	-1.77×10^0	−2.02
C_5H_8	-2.48×10^0	−1.61
β-Pinene	-1.19×10^{-1}	−1.04
SOA	5.00×10^0	2.74

Note: global burden (GB) and the mass values quoted are a yearly mean in gigagrams.
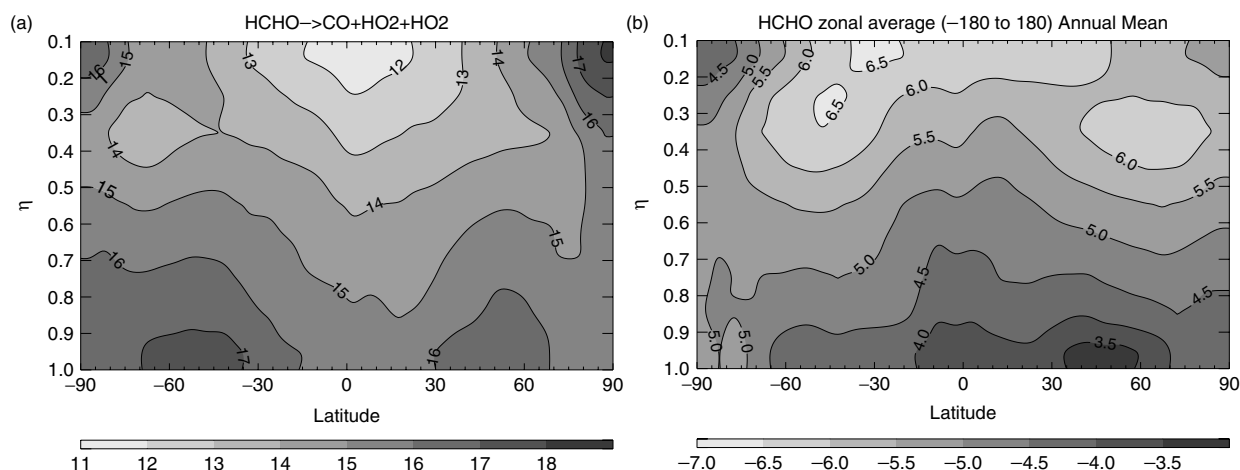
Figure 1. (a) Zonal mean percentage change in flux for the radical channel, JPL06 to CarJPL06, annual mean. (b) Zonal mean percentage change in formaldehyde concentration, JPL06 to CarJPL06, annual mean. Note: % change = [(CarJPL06 − JPL06)/JPL06] × 100.

The global concentration of H_2 (Table II) has reduced because of faster removal by OH and slower production via the molecular channel of HCHO photolysis. SOA produced by the partitioning of low-volatility products (Utembe *et al.*, 2009b) has increased overall because of their more efficient production from the oxidation of the precursor VOCs (isoprene, monoterpenes and aromatics). The percentage change in SOA is worthy of note, however, this magnitude of change is within the uncertainty of the representation. The formaldehyde concentration has been reduced on a global scale (Table II). The increased production from VOCs is balanced by the increased removal through reaction with OH. The increased photolysis on top of this thus leads to net removal of formaldehyde.

The changes, as percentages, in reaction flux for the radical channel as a zonal average are shown in Figure 1(a). This figure exhibits a vertical gradient, with the rate of reaction reducing with increasing altitude. As the VOC sources of HCHO are from the surface, a higher level of HCHO is expected at lower altitudes. As a result of the new photochemical data, HCHO is removed more rapidly from the atmosphere by faster photolysis. Therefore, the relative decrease in HCHO concentration is greatest at the top of the model domain (Figure 1(b)) and thus the rate of each photolysis reaction is reduced most at the top of the domain. This manifests itself as a reduction in the percentage increase with altitude for the radical channel. The molecular channel has a reduced flux overall with the greatest reduction in flux at the top of the troposphere. In the UT, the flux in the radical channel has increased most towards the poles because the higher wavelength threshold of the radical channel is more significant at higher solar zenith angles.

The global ozone concentration only changes by 0.03% (Table I). However, the plotted data in Figure 2(a) show that the increase in ozone in February over polluted regions is between 0.8 and 1.2 ppb between runs. February is used as a representative of a winter month in the northern hemisphere where there are shorter hours of daylight and higher solar
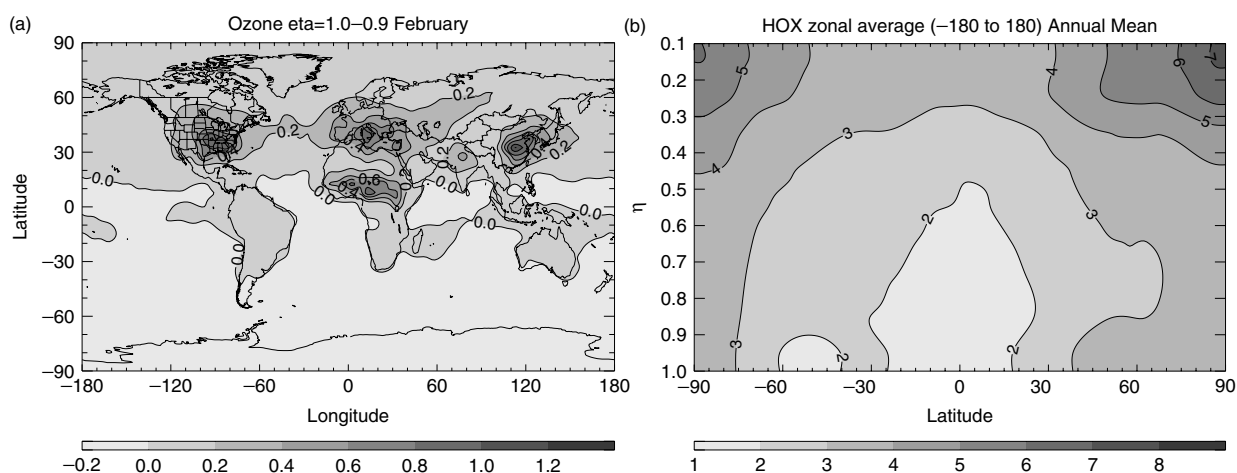

Figure 2. (a) Ground level mixing ratio change in ppb of ozone in February between JPL06 and CarJPL06. (b) Zonal mean percentage change in HO$_x$ concentration, JPL06 to CarJPL06, annual mean. Note: % change = [(CarJPL06 − JPL06)/JPL06] × 100.
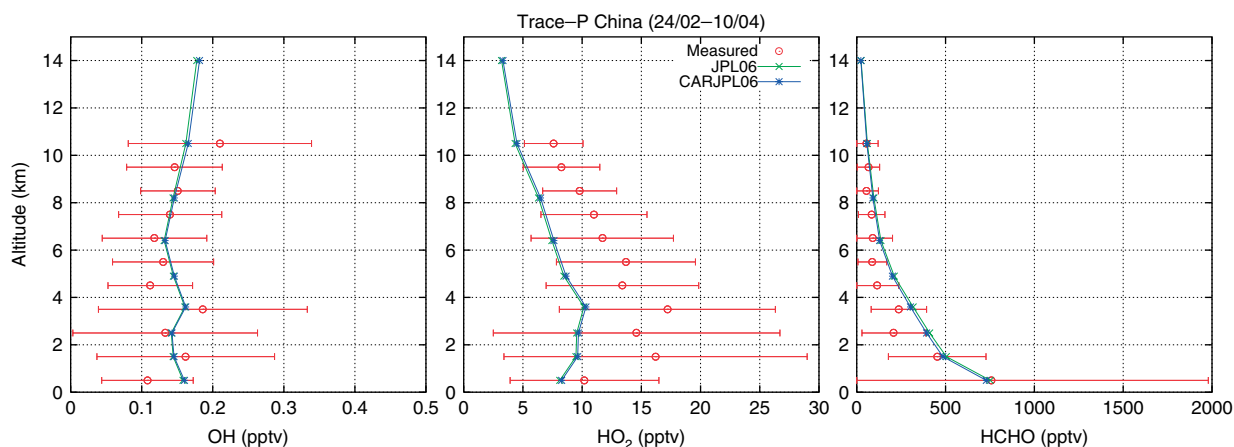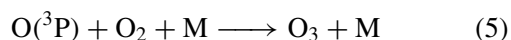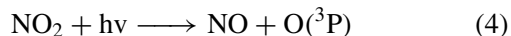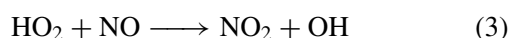
Figure 3. Comparison of OH, HO$_2$ and HCHO with airborne measurements taken from the data collection by Emmons *et al.* (2000). Red circles represent the mean of the measurements with error bars being a standard deviation in either direction. Green star and line represent the modelled value for run JPL06. Blue star and line represent the modelled value for run CarJPL06.

zenith angles relative to summer. HO$_2$ is predominantly produced when OH is oxidised by VOCs and via the photolysis of formaldehyde. At higher solar zenith angles, formaldehyde plays a more important role in HO$_2$ production relative to OH oxidation. The increased importance of the radical channel (run CAR-JPL06) of photolysis results greater in HO$_2$ production. Ozone is produced because of an increase in HO$_2$ via reactions (3–5).

$$HO_2 + NO \longrightarrow NO_2 + OH \qquad (3)$$

$$NO_2 + h\nu \longrightarrow NO + O(^3P) \qquad (4)$$

$$O(^3P) + O_2 + M \longrightarrow O_3 + M \qquad (5)$$

The increase in ozone ranging from 0.8 to 1.2 ppb is not observed in the summer months because the HO$_2$ production is dominated by OH oxidation. Therefore, the effect of formaldehyde on ozone production is greatest in the winter months with its significance gradually declining as summer approaches.

Figure 2(b) shows the zonal profile for the change in HO$_x$ concentration. HO$_x$ levels are increased most towards the top of the model. The largest increase in HO$_x$ at the ground level is in the northern mid to high latitudes between 40–90°N and 75–90°S in the southern hemisphere, with a change between 3 and 4%. The northern hemisphere has a greater change in HO$_x$ because the emissions of HCHO precursors from anthropogenic sources are greatest between 30 and 60°N. The largest increase at the top of the troposphere is towards the poles, because HO$_x$ production from HCHO is more significant at high-solar zenith angles. Overall, in the UT, there is an increase of 6% for HO$_2$ and 5% for OH. These are modest changes, but are in keeping with the idea that several precursors contribute to the HO$_x$ discrepancies between models and measurements. Of the HO$_x$ produced by acetone, alkyl peroxides and formaldehyde in the top level of the model approximately 85% is produced via formaldehyde photolysis. However, it must be made

clear that acetone and some of the alkyl peroxides are oxidised to formaldehyde in the photolytic mechanism and contribute to this 85%. The remaining 15% of HO$_x$ from these sources is via direct production from ROOH photolysis and from acetone prior to formaldehyde formation.

As a result of the changes in the formaldehyde *J*-values, a significant decrease was noted in the photochemical source strength for H$_2$ and subsequently in its global burden. Apart from direct emissions, photochemical production is the largest source term for this trace gas Simmonds *et al.* (2000).

4. Measurement comparison

Figure 3 shows the model and measurement data for the vertical profiles of the OH, hydroperoxy radical and formaldehyde off the coast of China during Trace-P. These measurements are for one aircraft campaign but give an indication of the significance of the updated photolysis parameters. The model is capable of recreating the vertical profile observed in these measurements and most values fall within the measurement error bars. The OH and HO$_2$ have increased most significantly towards the top of the model, 12 km and higher, moving the model closer to the mean of the measurements. The reductions in formaldehyde also move the model closer to the measured values. Figure 3 clearly shows that the formaldehyde photolysis data are not the major cause of discrepancies between model and measurements with regards to UT HO$_x$, however, it is a worthy update to current CTMs.

5. Conclusions

A global tropospheric CTM has been used to explore the changes in tropospheric trace gases resulting from recently reported photochemical parameters for

formaldehyde photolysis. We performed three simulations using formaldehyde photochemical data from DeMore (1992), Sander *et al.* (2006) and Gorrotxategi Carbajo *et al.* (2008). The percentages of formaldehyde removal via photolysis are calculated to be 60.9, 62.0 and 63.4%, respectively. The branching to the radical channel is more significant, with 23.2, 33.5 and 38.1% of formaldehyde global removal for the runs JPL92, JPL06 and CarJPL06, respectively. Global levels of OH and HO_2 are simulated to be 1.41 and 2.51% higher for the CarJPL06 than for the JPL06 runs. HO_x levels are increased most towards the top of the troposphere and the poles, making formaldehyde a more significant source of UT HO_x than previously thought. The increased HO_x leads to a faster destruction of VOCs, with decreases of 0.21, 2.02 and 1.61% in global mixing ratios of methane, benzene and isoprene, respectively. Globally, the computed ozone levels increase by 0.03%. Ozone over polluted areas of the northern hemisphere is found to be relatively unaffected in July and August. However, during February, as shown in Figure 2(a), when there are longer periods of higher solar zenith angles, there is a 0.8- to 1.2-ppb increase in ozone mixing ratios over the most polluted areas.

Acknowledgements

References

Andreae M, Merlet P. 2001. Emission of trace gases and aerosols from biomass burning. *Global Biogeochemical Cycles* **15**: 955–966.

Atkinson R, Baulch DL, Cox RA, Crowley JN, Hampson RF, Hynes RG, Jenkin ME, Rossi MJ, Troe J. 2006. Evaluated kinetic and photochemical data for atmospheric chemistry: volume II – gas phase reactions of organic species. *Atmospheric Chemistry and Physics* **6**: 3625–4055.

Brune WH. 1998. Airborne in situ OH and HO2 observations in the cloud-free troposphere and stratosphere during SUCCESS. *Geophysical Research Letters* **25**: 1701–1704.

Collins W, Stevenson D, Johnson C, Derwent R. 1997. Tropospheric ozone in a global-scale three-dimensional Lagrangian model and its response to NO$_X$ emission controls. *Journal of Atmospheric Chemistry* **26**: 223–274.

Collins WJ, Stevenson DS, Johnson CE, Derwent RG. 1999. Role of convection in determining the budget of odd hydrogen in the upper troposphere. *Journal of Geophysical Research-Atmospheres* **104**: 26927–26941.

Colomb A, Williams J, Crowley J, Gros V, Hofmann R, Salisbury G, Klupfel T, Kormann R, Stickler A, Forster C. 2006. Airborne measurements of trace organic species in the upper troposphere over Europe: the impact of deep convection. *Environmental Chemistry* **3**: 244.

Crawford J, Davis D, Olson J, Chen G, Liu S, Gregory G, Barrick J, Sachse G, Sandholm S, Heikes B. 1999. Assessment of upper tropospheric HOx sources over the tropical Pacific based on NASA GTE/PEM data: net effect on HOx and other photochemical parameters. *Journal of Geophysical Research-Atmospheres* **104**: 255–273.

DeMore WB. 1992. *Chemical Kinetics and Photochemical Data for Use in Stratospheric Modeling: Evaluation Number 10*. JPL Publication, 97-4. National Aeronautics and Space Administration, Jet Propulsion Laboratory, California Institute of Technology: CA, USA.

Derwent RG, Stevenson DS, Doherty RM, Collins WJ, Sanderson MG, Johnson CE. 2008. Radiative forcing from surface NO$_x$ emissions: spatial and seasonal variations. *Climatic Change* **88**: 385–401.

Emmons LK, Hauglustaine DA, Müller JF, Carroll MA, Brasseur GP, Brunner D, Staehelin J, Thouret V, Marenco A. 2000. Data composites of airborne observations of tropospheric ozone and its precursors. *Journal of Geophysical Research-Atmospheres* **105**: 497–538.

Fried A, Olson JR, Walega JG, Crawford JH, Chen G, Weibring P, Richter D, Roller C, Tittel F, Porter M. 2008. Role of convection in redistributing formaldehyde to the upper troposphere over North America and the North Atlantic during the summer 2004 INTEX campaign. *Journal of Geophysical Research* **113**: D17306.

Gorrotxategi Carbajo P, Smith SC, Holloway AL, Smith CA, Pope FD, Shallcross DE, Orr-Ewing AJ. 2008. Ultraviolet photolysis of HCHO: absolute HCO quantum yields by direct detection of the HCO radical photoproduct. *The Journal of Physical Chemistry A* **112**: 12437–12448.

Granier C, Lamarque J, Mieville A, Muller J, Olivier J, Orlando J, Peters J, Petron G, Tyndall S, Wallens S. 2005. *POET: A Database of Surface Emissions of Ozone Precursors*. Available at: http://www.aero.jussieu.fr/projet/ACCENT/POET.php. Accessed 2009.

Henze D, Seinfeld J, Ng N, Kroll J, Fu T, Jacob D, Heald C. 2008. Global modeling of secondary organic aerosol formation from aromatic hydrocarbons: high- vs. low-yield pathways. *Atmospheric Chemistry and Physics* **8**: 2405–2420.

Jaeglé L, Jacob DJ, Brune WH, Wennberg PO. 2001. Chemistry of HOx radicals in the upper troposphere. *Atmospheric Environment* **35**: 469–489.

Jenkin M, Watson L, Utembe S, Shallcross D. 2008. A Common Representative Intermediates (CRI) mechanism for VOC degradation. Part 1: gas phase mechanism development. *Atmospheric Environment* **42**: 7185–7195.

Logan JA, Prather SC, Wofsy SC, McElroy MB. 1981. Tropospheric chemistry: a global perspective. *Journal of Geophysical Research* **86**: 7210–7254.

Meller R, Moortgat GK. 2000. Temperature dependence of the absorption cross sections of formaldehyde between 223 and 323 K in the wavelength range 225–375 nm. *Journal of Geophysical Research* **105**: 7089–7102.

Penner J, Lister D, Griggs D, Dokken D, Mc-Farland M. 1999. IPCC special report on aviation and the global atmosphere. Technical report, Intergovernmental Panel on Climate Change. Cambridge University Press: New York.

Sander SP, Golden DM, Kurylo MJ, Moorgat GK, Wine PH, Ravishankara AR, Kolb CE, Molina MJ, Finlayson-Pitts BJ, Huie RE, Orkin VL. 2006. *Chemical Kinetics and Photochemical Data for Use in Atmospheric Studies: Evaluation Number 15*. NASA JPL: Publications 06-2.

Simmonds PG, Derwent RG, O'Doherty S, Ryall DB, Steele LP, Langenfelds RL, Salameh P, Wang HJ, Dimmer CH, Hudson LE. 2000. Continuous high-frequency observations of hydrogen at the Mace Head baseline atmospheric monitoring station over the 1994–1998 period. *Journal of Geophysical Research-Atmospheres* **105**: 12105–12121.

Smith CA, Pope FD, Cronin B, Parkes CB, Orr-Ewing AJ. 2006. Absorption cross sections of formaldehyde at wavelengths from 300 to 340 nm at 294 and 245 K. *The Journal of Physical Chemistry A* **110**: 11645–11653.

Utembe SR, Cooke MC, Archibald AT, Jenkin ME, Derwent RG, Shallcross DE. 2009a. Using a reduced Common Representative Intermediates (CRIv2-R5) mechanism to simulate tropospheric ozone in a 3-D Lagrangian chemistry transport model. *Atmospheric Environment*. in press.

Utembe SR, Watson LA, Shallcross DE, Jenkin ME. 2009b. A Common Representative Intermediates (CRI) mechanism for VOC degradation. Part 3: development of a secondary organic aerosol module. *Atmospheric Environment* **43**: 1982–1990.

Watson L, Shallcross D, Utembe S, Jenkin M. 2008. A Common Representative Intermediates (CRI) mechanism for VOC degradation. Part 2: gas phase mechanism reduction. *Atmospheric Environment* **42**: 7196–7204.